

Spin-polaron model: Transport properties of EuB_6

Jayita Chatterjee, Unjong Yu, and B. I. Min

Department of Physics, Pohang University of Science and Technology, Pohang 790-784, Korea

(Received 14 October 2003; revised manuscript received 2 February 2004; published 23 April 2004; corrected 12 July 2004)

To understand anomalous transport properties of EuB_6 , we have studied the spin-polaron Hamiltonian incorporating the electron-magnon and electron-phonon interactions. Assuming a strong exchange interaction between carriers and the localized spins, the electrical conductivity is calculated. The temperature and magnetic-field dependences of the resistivity of EuB_6 are well explained. At low temperature, magnons dominate the conduction process, whereas the lattice contribution becomes significant at very high temperature due to the scattering with the phonons. Large negative magnetoresistance near the ferromagnetic transition is also reproduced as observed in EuB_6 .

DOI: 10.1103/PhysRevB.69.134423

PACS number(s): 75.47.Pq, 72.10.Di, 71.38.-k

Hexaboride compounds have been studied extensively for their unusual transport and magnetic properties. Among those, EuB_6 has attracted special interest due to its exotic magnetic properties, such as two consecutive phase transitions at low temperature (15.5 K and 12.6 K), very low carrier density ($\sim 10^{20} \text{ cm}^{-3}$), metallic ferromagnetism below T_c , and large negative colossal magnetoresistance at the transition of 15 K.^{1,2} It was proposed that the higher transition temperature is a metallization temperature due to an increase in the number of itinerant electrons and the lower one is a bulk Curie temperature of long-range ferromagnetic (FM) order.² Sample dependence is an important issue in EuB_6 as it has a very small number of intrinsic carriers. The higher transition temperature is seen to be much more sample dependent than the lower one.²

Raman-scattering measurements^{3,4} indicated the spontaneous formation of magnetic polarons, involving FM clusters of Eu^{2+} spins just above T_c . It was conjectured³ that the transition at higher temperature arises from the mutual interaction between the magnetic moments and the conduction electrons which leads to the formation of bound magnetic polarons. The bound magnetic polaron corresponds to a composite object of localized charge carrier and its induced alignment in a background of local moments. On the other hand, Hirsch⁵ proposed a model that the magnetism of EuB_6 is driven by the effective mass reduction or the band broadening upon spin polarization. The origin of this effect is the bond-charge Coulomb repulsion which, in a tight-binding model, corresponds to the “off-diagonal” nearest-neighbor exchange and pair hopping matrix elements of the Coulomb interaction. But the parameters for the exchange and pair hopping considered in his model are unphysical and the Eu 4*f* states were treated as delocalized electrons in contrast to the band-structure results.⁶ The Ruderman-Kittel-Kasuya-Yosida interaction among the localized 4*f* electrons through itinerant electrons is also considered to be an origin of ferromagnetism in EuB_6 .⁷ More recently, a fluctuation-induced hopping model is proposed as a transport mechanism for the spin polaron in a paramagnetic background of fluctuating local moments.⁸ In this case, temperature dependence of the resistivity is obtained to be proportional to $T^{5/2}$ for $k_B T \gtrsim J_{\text{FM}}$ and to T for $k_B T \gg J_{\text{FM}}$, where J_{FM} is coupling between the local moments. They claimed that this transport

mechanism is valid for the high-temperature phase of EuB_6 . However, no $T^{5/2}$ behavior is observed and, moreover, the crossover temperature is too high to be applicable to EuB_6 .

The diverse properties of EuB_6 are expected to come primarily from the exchange interactions between the carriers and Eu^{2+} 4*f* local moments. Indeed, the large energy and field dependence of the spin-flip Raman-scattering peak³ reflects the substantial FM exchange interaction ($J_{cf} \sim 0.1 \text{ eV}$) between the carrier and the Eu^{2+} spins in EuB_6 . The magnetic polaron formation is favored by the large ferromagnetic J_{cf} ,⁴ as a trapped charge lowers its energy by polarizing the local moments of Eu^{2+} .

The low-carrier density magnetic systems such as EuB_6 share many properties with the colossal magnetoresistance manganites, such as the insulator-metal transition concomitant with the FM transition, large negative magnetoresistance, and the formation of magnetic clusters near T_c . Distinctly from manganites, however, Eu-based systems do not manifest the structural complexities originating from the strong electron-lattice coupling associated with Jahn-Teller effect. Due to the structural simplicity, EuB_6 is an ideal system for investigation of the interplay between magnetic and transport properties. An essential aspect for a theoretical understanding of the properties of EuB_6 is the temperature dependences of the resistivity. So it would be of great interest to study the temperature and field dependence of resistivity of EuB_6 . For this purpose, we consider the spin-polaron Hamiltonian taking into account the magnetic excitations (magnons in the linear spin-wave approximation) together with lattice excitations (phonons),

$$\begin{aligned}
 H = & - \sum_{\langle i,j \rangle, \sigma} t c_{i\sigma}^\dagger c_{j\sigma} + \sum_q \omega_q a_q^\dagger a_q + \sum_p \Omega_p b_p^\dagger b_p \\
 & - \sum_{i,q} \frac{J_q}{2} e^{iq \cdot \vec{R}_i} (c_{i\uparrow}^\dagger c_{i\downarrow} a_{-q}^\dagger + c_{i\downarrow}^\dagger c_{i\uparrow} a_q^\dagger) \\
 & + \sum_{i,p} g_p e^{ip \cdot \vec{R}_i} (c_{i\uparrow}^\dagger c_{i\uparrow} + c_{i\downarrow}^\dagger c_{i\downarrow}) (b_p^- + b_{-p}^\dagger), \quad (1)
 \end{aligned}$$

where $c_{i\sigma}$ is the annihilation operator for the conduction electron with spin σ at site i , a_q^- and b_p^- are the annihilation

operators for a localized spin (magnon) with momentum \vec{q} and for the phonons with wave vector \vec{p} , respectively, and $\omega_{\vec{q}}$ and $\Omega_{\vec{p}}$ are the magnon and phonon frequencies, respectively. $\omega_{\vec{q}} \sim J_{FM} S$ where J_{FM} is the direct FM exchange interaction between Eu 4f spins (S). The last two terms are the interaction between the itinerant electrons and localized spins and that between the local density of the carrier (n_i) and localized charge vibrations (phonons), respectively. The non-spin-flip-interaction term $[S^z(n_{i\uparrow} - n_{i\downarrow})]$ which just shifts the on-site energy is not considered, as we are interested only in the transport properties. Without loss of generality, the Coulomb interaction can be neglected in the very low carrier density limit.

In EuB_6 , it was observed that clusters of Eu^{2+} spins are formed via the strong ferromagnetic c - f exchange interaction.³ Hence one can assume a strong exchange coupling which induces the locally ferromagnetically ordered spin clusters in the ground state. Formation of magnetic polarons is possible in the low-carrier-density magnetic system if the degrees of spin disorder is sufficient to localize the carrier, but not too high to prevent the local FM alignment.⁴ As for the electron-phonon (e -ph) interaction, the study of boron isotope effect suggests that the polarons formed in EuB_6 are predominantly magnetic, with a negligible lattice contribution.⁴ It is, however, not so certain that the magnetic polaron in EuB_6 do not couple to the lattice degrees of freedom of Eu ions. Further, thermal-conductivity measurement on EuB_6 reveals that the e -ph scattering is strongly favored below T_c to describe the T^2 variation of the thermal conductivity.⁹ Therefore, to explore the role of lattice in the magnetic polaron formation, it is worthwhile to consider the e -ph interaction in the Hamiltonian.

To decouple the electron-magnon interaction term, we employ the following canonical transformation:

$$\tilde{H} = e^{R_1} H e^{-R_1},$$

$$R_1 = \sum_{i,\vec{q}} \frac{J_{\vec{q}}}{\omega_{\vec{q}}} e^{i\vec{q} \cdot \vec{R}_i} (c_{i\uparrow}^\dagger c_{i\downarrow} + c_{i\downarrow}^\dagger c_{i\uparrow}) (a_{\vec{q}}^- - a_{-\vec{q}}^\dagger). \quad (2)$$

In the presence of e -ph coupling, spread and depth of lattice deformation can be studied by using the Lang-Firsov (LF) transformation,¹⁰

$$\tilde{H}_{\text{LF}} = e^{R_2} \tilde{H} e^{-R_2},$$

$$R_2 = - \sum_{j,\vec{p}} \frac{g_{\vec{p}}}{\Omega_{\vec{p}}} e^{i\vec{p} \cdot \vec{R}_j} n_j (b_{\vec{p}}^- - b_{-\vec{p}}^\dagger). \quad (3)$$

Note that, for weak to intermediate e -ph coupling, the variational LF transformation¹¹ would give more satisfactory results than LF transformation. In the present work, we consider the LF transformation for simplicity.

As a result, the transformed Hamiltonian becomes,

$$\begin{aligned} \tilde{H}_{\text{LF}} = & - \sum_{\langle i,j \rangle, \sigma} t [\cosh(x_i - x_j) X_i^\dagger X_j c_{i,\sigma}^\dagger c_{j,\sigma} + \sinh(x_i - x_j) \\ & \times X_i^\dagger X_j c_{i,\sigma}^\dagger c_{j,-\sigma}] + \sum_{\vec{q}} \omega_{\vec{q}} a_{\vec{q}}^\dagger a_{\vec{q}} + O(n_{i\uparrow} n_{i\downarrow}) \\ & + O(c_{i\uparrow}^\dagger c_{m\downarrow}^\dagger c_{m\uparrow} c_{i\downarrow}) + \sum_{\vec{p}} \Omega_{\vec{p}} b_{\vec{p}}^\dagger b_{\vec{p}} - \sum_{i,p} \frac{g_{\vec{p}}^2}{\Omega_{\vec{p}}} n_i \\ & - \sum_{i,j,\vec{p}}^{i \neq j} \frac{g_{\vec{p}}^2}{\Omega_{\vec{p}}} n_i n_j e^{i\vec{p} \cdot (\vec{R}_i - \vec{R}_j)}, \end{aligned} \quad (4)$$

where

$$x_i = \sum_{\vec{q}} \frac{J_{\vec{q}}}{\omega_{\vec{q}}} e^{i\vec{q} \cdot \vec{R}_i} (a_{\vec{q}}^- - a_{-\vec{q}}^\dagger), \quad (5)$$

$$X_i = \exp \left[\sum_{\vec{p}} \frac{g_{\vec{p}}}{\Omega_{\vec{p}}} e^{i\vec{p} \cdot \vec{R}_i} (b_{\vec{p}}^- - b_{-\vec{p}}^\dagger) \right]. \quad (6)$$

The magnon part remains unchanged after the transformations. In the transformed Hamiltonian, only the hopping term contains nonlinear functions of spin-wave operators. As we are interested in the transport properties in the very low carrier density limit, we will not consider the renormalized interactions between carriers. To calculate the electrical conductivity, dynamics of $\cosh(x_i - x_j) X_i^\dagger X_j$ and $\sinh(x_i - x_j) X_i^\dagger X_j$ in the hopping term of Eq. (4) should be properly treated. At low temperature, transport is described by an effective bandwidth with a background of magnons and phonons. The effective mass of the carrier increases as a result of the interaction with the magnons. The effect of the background is included by calculating the thermal average of $\cosh(x_i - x_j) X_i^\dagger X_j$ and $\sinh(x_i - x_j) X_i^\dagger X_j$.

In conduction, there are two independent processes: elastic and inelastic. For the elastic conduction process, thermal average of the terms mentioned above is calculated as in the conventional polaron problem,¹² assuming all magnons and phonons to be independent:

$$\begin{aligned} \langle \cosh(x_i - x_j) X_i^\dagger X_j \rangle = & \exp[-|V_{\vec{q}}|^2 N_{\vec{q}}^{\text{mag}}] \exp[-|U_{\vec{p}}|^2 N_{\vec{p}}^{\text{ph}}] \\ & \times \exp[-\frac{1}{2}(|V_{\vec{q}}|^2 + |U_{\vec{p}}|^2)], \end{aligned} \quad (7)$$

and $\langle \sinh(x_i - x_j) X_i^\dagger X_j \rangle = 0$. Here $N_{\vec{q}}^{\text{mag}}$ and $N_{\vec{p}}^{\text{ph}}$ are the magnon and phonon numbers, respectively,

$$\begin{aligned} N_{\vec{q}}^{\text{mag}} = & \{ \exp[\omega_{\vec{q}} / (k_B T)] - 1 \}^{-1}, \\ N_{\vec{p}}^{\text{ph}} = & \{ \exp[\Omega_{\vec{p}} / (k_B T)] - 1 \}^{-1}, \end{aligned} \quad (8)$$

and

$$V_q^- = \frac{J_q^-}{\omega_q^-} e^{i\vec{q} \cdot \vec{R}_i} (1 - e^{i\vec{q} \cdot \vec{\delta}}),$$

$$U_p^- = \frac{g_p^-}{\Omega_p^-} e^{i\vec{p} \cdot \vec{R}_i} (1 - e^{i\vec{p} \cdot \vec{\delta}}), \quad (9)$$

where $\vec{\delta} = \vec{R}_i - \vec{R}_j$ and $\langle \dots \rangle$ denotes the thermal average. The temperature dependence in the above thermal average comes only through N_q^{mag} and N_p^{ph} . If we assume at finite temperature that the metallic conduction of the elastic process σ_e is inversely proportional to the effective mass¹³ and the effective mass is inversely proportional to the effective bandwidth, then

$$\sigma_e(T) \propto \langle t \cosh(x_i - x_j) X_i^\dagger X_j \rangle. \quad (10)$$

For the inelastic process, the conduction is provided by the incoherent hopping with emitting and absorbing the magnons and phonons. The conductivity is given by the Kubo formula,¹²

$$\sigma_{\text{in}} = ne^2 w \delta^2 / (3k_B T), \quad (11)$$

where n is density of mobile carriers, and w is the transition probability rate given by the Fermi golden rule,

$$w = (t^2 / \hbar \Delta) \exp(-\Delta / k_B T), \quad (12)$$

with the activation energy $\Delta = \frac{1}{4} (\sum_q \omega_q^- |V_q^-|^2 + \sum_p \Omega_p^- |U_p^-|^2)$. For simplicity, if we consider single magnon (ω) and phonon (Ω) frequency, the total conductivity is given by the sum of two independent processes,

$$\sigma(T) / \sigma(0) = \exp[-\alpha N(\omega) - \beta N(\Omega)] + [b^2 / (3\Delta k_B T)] \times \exp(-\Delta / k_B T), \quad (13)$$

where $\alpha = \sum_q |V_q^-|^2$, $\beta = \sum_p |U_p^-|^2$, $b = et \delta \sqrt{n / \hbar \sigma(0)}$, and $\sigma(0)$ is the zero-temperature conductivity.

For numerical calculation, we consider $\omega \sim T_c$. As for Ω , since no inelastic neutron scattering measurements have been reported on EuB_6 , we tentatively use the renormalized frequency based on the Einstein phonon frequency for LaB_6 .¹⁴ If we assume $\Omega = 168$ K for the localized mode of Eu^{2+} ion, the model calculation reproduces the experimental features. The activation energy is a function of ω and Ω , and also a function of J_{cf} and e -ph coupling. We observed that nature of the resistivity is sensitive to the energy parameters Δ and b . The average distortion around Eu site is more than an order of magnitude smaller than that in the perovskites,¹⁵ and so we choose β to be much less than α .

Figure 1 provides the calculated resistivity (normalized to $T=0$) as a function of temperature. The calculated resistivity describes well the qualitative features of the experimental resistivity.¹⁶⁻¹⁹ For comparison with the experimental data, we have multiplied our results by an arbitrary factor and

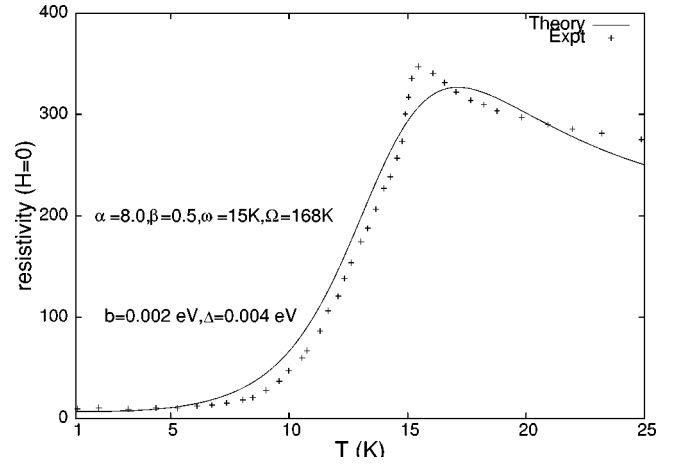


FIG. 1. The normalized resistivity (arbitrary units) for EuB_6 in the low-temperature region with $\omega = 15$ K, $\Omega = 168$ K, $\alpha = 8.0$, $\beta = 0.5$, $\Delta = 0.004$ eV, $b = 0.002$ eV. “+” symbols represent the experimental data in $\mu\Omega$ cm (Ref. 17).

found very satisfactory agreement with the experimental results. In the present model, the resistivity peak near 15 K signifies the crossover from a high-temperature insulating state with localized and isolated carriers (magnetic polarons) to a low-temperature conducting state resulting from the overlap of the magnetic polarons. Polaron overlap is marked by the rapid drop in resistivity at the transition. Consideration of only the electron-magnon interaction in the present model can reproduce the resistivity peak around 15 K. However, the inclusion of phonons within this model makes the agreement better. At very low temperature, the contribution of magnons to the conductivity is more important than that of phonons. With increasing temperature, the band conduction dominates with enhanced effective mass of the carrier so that the resistivity increases very rapidly. In contrast, at very high temperature, the role of the lattice effect becomes significant due to the scattering with the phonons,⁹ where the incoherent hopping dominates.

Now let us investigate the effect of the external magnetic field on the transport. One can include the effect of the external magnetic field H for FM magnons by replacing the magnon frequency ω_q^- by $(\omega_q^- + g_{\text{eff}} \mu_B H)$, where g_{eff} is the effective g factor for the localized spins of Eu^{2+} . $g_{\text{eff}} (= g^* + J_{cf} \chi / g \mu_B^2 x_c)$ takes into account the enhanced effective field arising from the exchange interaction between the carriers and $\text{Eu-4}f$ local moments in the presence of the magnetic field. Here g^* is the intrinsic g factor for the $\text{Eu-4}f$ spin, χ and g are the susceptibility and the g factor for the conduction electrons, respectively, and x_c is the concentration of conduction electron. Taking the temperature-independent Pauli paramagnetic susceptibility for χ which is given by the density of states $N(E_F)$ of conduction electrons²⁰ and $x_c = 0.01$ per unit cell,^{2,21} one can estimate the value of g_{eff} to be nearly equal to 6. Then, with the above field dependent ω_q^- , the experimental results of large magnetoresistance can be achieved.

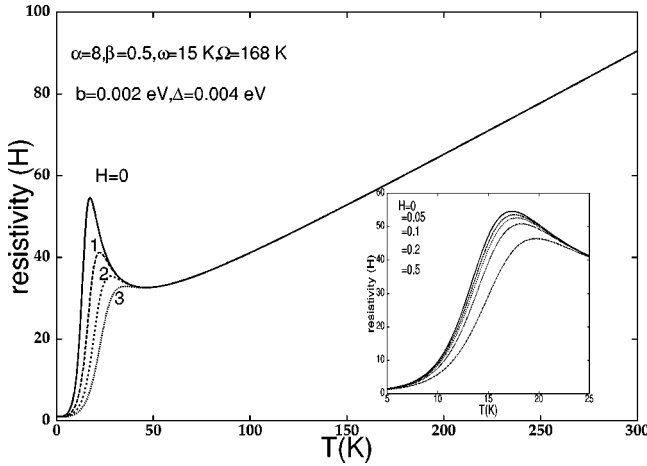


FIG. 2. Normalized resistivity vs temperature T (K) for different magnetic fields H (in tesla). The inset shows the low-temperature variation of resistivity.

The temperature dependence of the electrical resistivity with varying the external magnetic field is presented in Fig. 2. The field and temperature dependences of the electrical resistivity reveal that the charge transport is strongly correlated with the higher transition temperature.² In the presence of magnetic field, the transition is broadened and shifted to higher temperature. In the inset shown is the resistivity in the low-temperature region with varying the external magnetic field ranging from 0.05 to 0.5 T. At zero field, the resistance drops sharply just above the transition temperature. This resistivity peak is suppressed by the magnetic field in good agreement with the observation.²

In Fig. 3, we plot the magnetoresistance ($MR = [\rho(H) - \rho(0)]/\rho(0)$) predicted by the present model as a function of temperature. With increasing temperature, a large negative contribution to MR appears. We obtain the negative MR even at temperatures higher than T_c , which is consistent with the experiment.¹⁶ Inset of Fig. 3 provides the normalized MR at $T = T_c$ (15 K) as a function of the external mag-

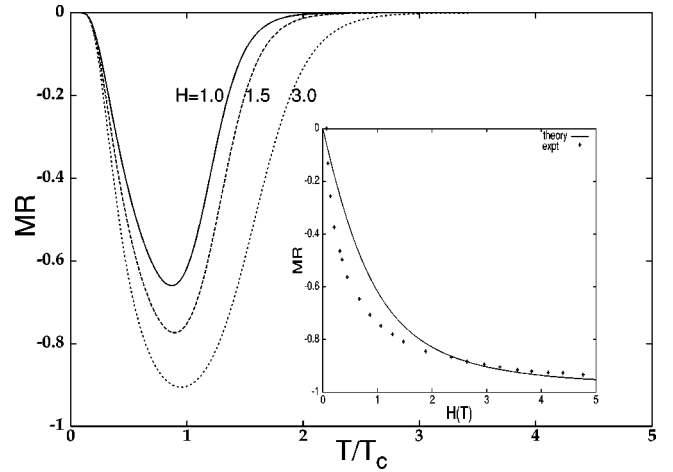


FIG. 3. Normalized magnetoresistance (MR) vs temperature (T/T_c with $T_c = 15$ K) for different values of the magnetic field (in tesla). The same parameters as in Fig. 1 are used. Inset: MR vs H (in tesla) at $T = 15$ K. “+” symbols represent the experimental data (Ref. 17).

netic field. A large negative MR near the FM transition, as depicted in the inset, is indeed observed in EuB_6 .¹⁷ The MR approaches -1 in the high-field limit, reflecting that the zero-field resistivity is completely suppressed, which is in excellent agreement with experimental features.

In conclusion, we have proposed the model which accounts qualitatively well for several anomalous transport properties observed in EuB_6 . The strong exchange interaction (J_{cf}) and the FM magnons in the present model can reproduce the temperature and magnetic-field dependences of the resistivity in EuB_6 . Large negative MR occurs even at temperatures higher than T_c , which is consistent with experiments.

This work was supported by the KOSEF through the eSSC at POSTECH and in part by the KRF (Grant No. KRF-2002-070-C00038).

¹T. Fujita, M. Suzuki, and Y. Ishikawa, *Solid State Commun.* **33**, 947 (1980).

²S. Süllow, I. Prasad, M.C. Aronson, S. Bogdanovich, J.L. Sarrao, and Z. Fisk, *Phys. Rev. B* **62**, 11 626 (2000).

³P. Nyhus, S. Yoon, M. Kauffman, S.L. Cooper, Z. Fisk, and J. Sarrao, *Phys. Rev. B* **56**, 2717 (1997).

⁴C.S. Snow, S.L. Cooper, D.P. Young, Z. Fisk, A. Comment, and J.-P. Ansermet, *Phys. Rev. B* **64**, 174412 (2001).

⁵J.E. Hirsch, *Phys. Rev. B* **59**, 436 (1999).

⁶S. Massidda, A. Continenza, T.M. de Pascale, and R. Monnier, *Z. Phys. B: Condens. Matter* **102**, 83 (1997).

⁷J.C. Cooley, M.C. Aronson, J.L. Sarrao, and Z. Fisk, *Phys. Rev. B* **56**, 14 541 (1997).

⁸L.G.L. Wegener and P.B. Littlewood, *Phys. Rev. B* **66**, 224402 (2002).

⁹P. Vonlanthen, S. Paschen, D. Pushin, A.D. Bianchi, H.R. Ott, J.L.

Sarrao, and Z. Fisk, *Phys. Rev. B* **62**, 3246 (2000).

¹⁰I.G. Lang and Y.A. Firsov, *Zh. Eksp. Teor. Fiz.* **43**, 1843 (1962) [*Sov. Phys. JETP* **16**, 1301 (1963)].

¹¹A.N. Das and S. Sil, *J. Phys.: Condens. Matter* **5**, 8265 (1993).

¹²G. D. Mahan, *Many-Particle Physics* (Plenum, New York, 1990).

¹³S. Zhang, *J. Appl. Phys.* **79**, 4542 (1996).

¹⁴D. Mandrus, B.C. Sales, and R. Jin, *Phys. Rev. B* **64**, 012302 (2001).

¹⁵C.H. Booth, J.L. Sarrao, M.F. Hundley, A.L. Cornelius, G.H. Kwei, A. Bianchi, Z. Fisk, and J.M. Lawrence, *Phys. Rev. B* **63**, 224302 (2001).

¹⁶C.N. Guy, S. von Molnar, J. Etourneau, and Z. Fisk, *Solid State Commun.* **33**, 1055 (1980).

¹⁷S. Süllow, I. Prasad, M.C. Aronson, J.L. Sarrao, Z. Fisk, D. Hristova, A.H. Lacerda, M.F. Hundley, A. Vigliante, and D.

- Gibbs, Phys. Rev. B **57**, 5860 (1998).
- ¹⁸Z. Fisk, D.C. Johnston, B. Cornut, S. von Molnar, S. Oseroff, and R. Calvo, J. Appl. Phys. **50**, 1911 (1979).
- ¹⁹J.-S. Rhyee, B.K. Cho, and H.-C. Ri, Phys. Rev. B **67**, 125102 (2003).
- ²⁰We used $N(E_F)=0.73/\text{eV}$ per unit cell obtained from the LDA band calculation. J. H. Shim (unpublished).
- ²¹S. Süllo, I. Prasad, S. Bogdanovich, M.C. Aronson, J.L. Sarrao, and Z. Fisk, J. Appl. Phys. **87**, 5591 (2000).